HOT JUPITERS AROUND YOUNG STARS

L. F. Yu[1] and J.-F. Donati[1]

Abstract. This conference paper presents the results of the MaTYSSE (Magnetic Topologies of Young Stars and the Survival of massive close-in Exoplanets) observation programme, regarding the search for giant exoplanets around weak-line T Tauri stars (wTTS), as of early 2017. The discoveries of two hot Jupiters (hJs), around V830 Tau and TAP 26, sun-like stars of respectively ∼2 Myr and ∼17 Myr, are summarized here. Both exoplanets seem to have undergone type-II migration (planet-disc interaction leading the orbit to narrow around the host) based on their low orbital eccentricity. The methods which were used are given more focus in the paper *Stellar activity filtering methods for the detection of exoplanets* in the present book.

Keywords: methods: statistical, stars: activity, stars: evolution, stars: imaging, stars: individual (V830 Tau, TAP 26), stars: magnetic fields, (stars:) planetary systems: formation, stars: pre–main-sequence, stars: rotation, stars: spots

1 Introduction

To improve the community's understanding of the formation and early evolution of solar-like planetary systems, we investigate the migration processes of hot Jupiters at the beginning of their life. Hot Jupiters are massive close-in exoplanets which have, according to the theory, formed beyond the ice line and then migrated inwards due to one of these interactions: planet-disc interaction which induces a fast (a few 0.1 Myr) and smooth (quasi circular orbit) migration, or planet-planet scattering where several already formed planets interact and one of them ends up on a highly eccentric orbit, progressively circularized by tidal effects (several ∼10 Myr). Due to their strong gravitational influence on the rest of the bodies in their system, constraining the migration process of hJs can help to elucidate the early orbital choreography of solar-like planetary systems.

The sample of the MaTYSSE (Magnetic Topologies of Young Stars and the Survival of massive close-in Exoplanets) programme, some 30+ solar-like stars of a few Myrs (33 weak-line Tauri stars – wTTS, whose disk has mostly dissipated, and 6 classical T Tauri stars – cTTS, which still have an accretion disk), therefore offers ideal targets to hunt for hJs and, in case of success, distinguish between these two processes. MaTYSSE aims at studying the role of the magnetic field in the early stages of a star's life (loss of the disc, formation of exoplanets) thanks to spectra in the optical bandwidth taken with the ESPaDOnS (Echelle SpectroPolarimetric Device for the Observation of Stars) and NARVAL instruments, mounted on the Canada France Hawaii Telescope (CFHT) and on the TBL (Télescope Bernard Lyot) respectively. The planet detection technique used here is the velocimetry method.

However, wTTSs are fast rotators (with periods of the order of the day) and thus have a high level of magnetic activity, which manifests itself in particular in a high brightness contrast on the photosphere. This contrast, added to the stellar rotation, induces distorsions in the line profiles of the stellar spectrum, which in turn add a jitter (called "activity jitter") in the stellar line-of-sight-projected velocity (radial velocity, RV), making it more difficult to detect a planet signature in the RV signal.

2 Methods

2.1 Spectra and radial velocity (RV)

The unpolarized (Stokes I) spectral lines of wTTSs, which are used to compute the stellar RV, are shaped by the Doppler effect, which causes a strong correlation between the location of spots on the surface of the

---

[1] IRAP, Université de Toulouse, CNRS, UPS, CNES, Toulouse, France

star (and therefore their local RV) and distorsions in the rotation-broadened line profiles. Assuming that the distorsions are the same in most spectral lines (each line being weighed by its equivalent width), Least-Squares Deconvolution (LSD) profiles have been generated for each spectrum in order to concentrate the information into one profile, the x-axis of which represents the local RV (see Fig. 1 for an illustration).

The RVs, in which one looks for a periodic signal in order to detect a planet, are computed as the centroid of the continuum-subtracted LSD profiles. Because of the brightness contrast and the stellar rotation, the RV signal one derives from a planetless wTTS is not constant and the resulting modulation, called activity jitter (typically of the order of 1 km s^{-1} of amplitude), follows the stellar rotation period (see Fig. 2).

The star's global motion, and in particular the hypothetical reflex motion it would have in the presence of a planet (typically of the order of 0.1 km s^{-1} of amplitude), does not change the shape of the line profiles, but shifts the whole spectrum according to the star's RV. As a consequence, the computed RV of the star is the sum of the activity jitter and of the actual stellar RV.

The aim of this study is to model the activity of each star in order to subtract its activity jitter from its RV curves and look for potential planet signatures in the filtered RVs.

2.2 Imaging and filtering process, example of wTTS TAP 26

This section explains the imaging and RV filtering process, using the case of wTTS TAP 26 as an illustration. The reader is invited to consult Yu et al. (2017) for a full in-depth explanation.

TAP 26 is a 17 Myr wTTS located in the Taurus region, with a 1.04±0.10 M$_\odot$ mass and a rotation period of 0.7135 d (see Table 1). Theoretical evolution models (Siess et al. 2000) suggest that its radiative core has reached a radius of at least half the stellar radius and that its magnetic field has started to evolve into a complex topology (Gregory et al. 2012).

29 observations, comprising both unpolarized (Stokes I) and circularly polarized (Stokes V) spectra, were taken with the ESPaDOnS spectropolarimeter, 16 in November 2015 and 13 in January 2016 (see Fig. 1 middle).
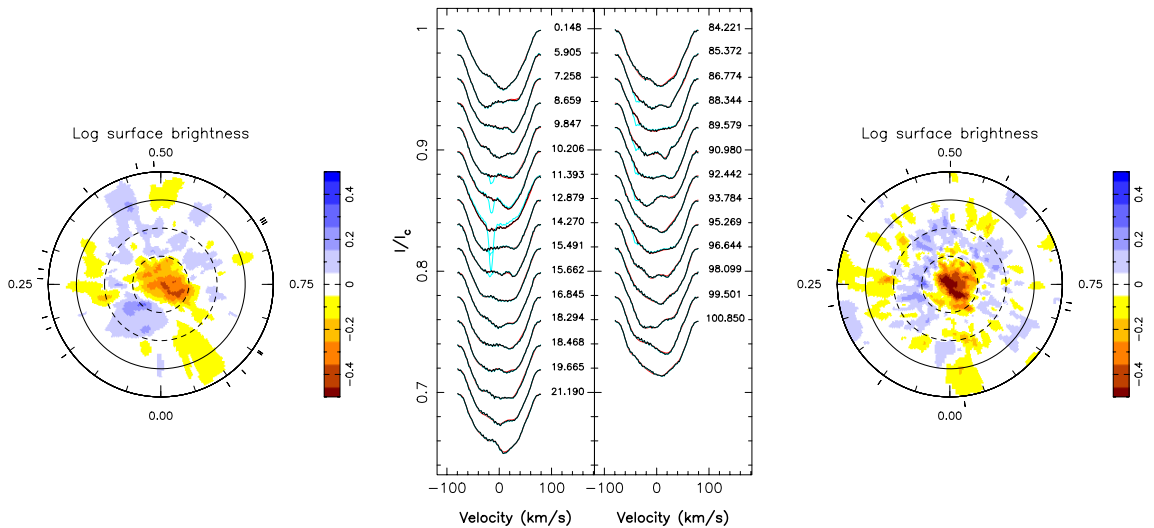

Fig. 1. Middle: maximum entropy fit (thin red lines) to the observed (thick black lines) Stokes I LSD profiles, with the 2015 Nov dataset on the left and the 2016 Jan dataset on the right (the Stokes I LSD profiles before the removal of lunar pollution are coloured in cyan). The rotational cycles are written beside their corresponding profiles, in concordance with Table 1 in Yu et al. (2017). **Left** and **right**: Flattened polar view of the surface brightness maps for the 2015 Nov dataset (left) and 2016 Jan dataset (right), with the equator, the 60°, 30° and -30° latitude parallels as solid and dashed black lines respectively. The colour scale indicates the logarithm of the relative brightness, with brown/blue areas representing cool spots/bright plages, and the outer ticks mark the phases of observation.

Zeeman-Doppler Imaging (ZDI, Donati & Brown 1997) was used to reconstruct the brightness and magnetic maps that generate the spectra which fit our LSD profiles down to noise level with the smallest amount of information. The maps are constituted of a mesh over the visible surface of the star (which depends on its inclination) where each cell has a local brightness value and the three components of the local magnetic field, which influence the local line profile through the Doppler and Zeeman effects. The synthesized line profile is

then integrated over the visible surface, taking into account the local radial velocity, causing Doppler broadening (dictated by the equatorial velocity and the inclination) and limb darkening. A sine-square latitudinal differential rotation can be considered in the fitting process.

The reconstructed brightness maps are displayed on Fig. 1 (left and right). Although the main brightness features remain similar between both observation epochs, the evolution of the surface brightness distribution in the span of a few months is noticeable. The activity jitter, derived from the synthetic profiles generated from the reconstructed brightness maps, is shown on Fig. 2 and exhibits a periodicity corresponding to stellar rotation, as well as some temporal evolution, due not only to differential rotation (visible within each observing epoch), but also to intrinsic variability (visible as a difference between both observing epochs).
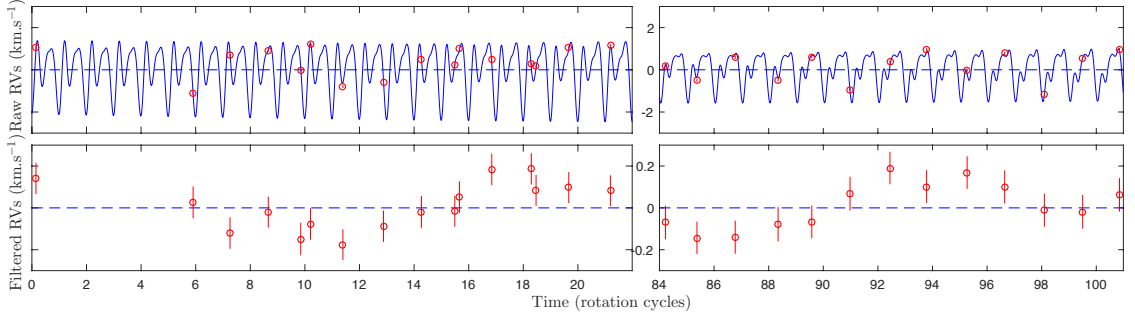

Fig. 2. Top: RV (in the stellar rest frame) of TAP 26 as a function of rotation phase, as measured from our observations (open circles) and predicted by the tomographic maps (blue line). **Bottom**: filtered RVs derived by subtracting the modelled activity jitter from the raw RVs, with a 10x zoom-in on the vertical axis.

After subtracting the activity jitter from the raw RVs (derived from the observed LSD profiles), several periods stand out in the filtered RV due to the observing window (see Fig. 3). However, the period with highest likelihood, at 13.41 d, has a false-alarm probability of 6×10^{-4}, confirming the presence of a periodic signal in the star's RVs, and therefore the presence of a planet. After subtracting the corresponding sine wave fit from the filtered RVs, the residual RVs have a rms of 51 m s^{-1}, which is close to noise level. Trying to fit a keplerian curve in the filtered RVs yields an eccentricity of 0.16±0.15, which favors the hypothesis of type II migration over planet-planet scattering. See Table 1 for the planet properties.
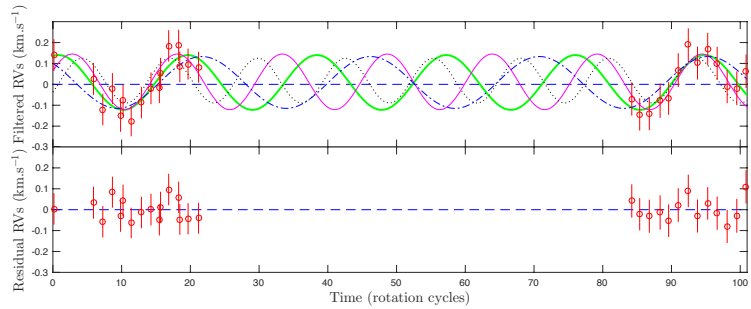

Fig. 3. Top: Filtered RVs of TAP 26 and four sine curves representing the best fits. The thick green curve represents the case $P_{\rm orb} = 18.80$ $P_{\rm rot} = 13.41$ d. **Bottom**: Residual RVs resulting from the subtraction of the best fit (green curve) from the filtered RVs.

Other methods were used to analyze the spectra and RV curves of TAP 26, which confirmed the periodicities detected in the filtered RVs with the method detailed above. Simulations were also conducted in order to verify that such periods were not generated by the filtering process (Yu et al. 2017).

3   MaTYSSE results

Two hJs around TTSs have been found within the MaTYSSE programme, their properties are found in Table 1.

The formation of hJs can therefore be as fast as a few million years. In both cases, the eccentricity was found to be negligible, favoring the hypothesis of type II migration over planet-planet scattering, with the fact

	V830 Tau (Donati et al. 2016)	**TAP 26** (Yu et al. 2017)
Age [Myr]	$\simeq$2.2	$\simeq$17
$M_\star$ [M$_\odot$]	1.00$\pm$0.05	1.04$\pm$0.10
$P_{\rm rot}$ [d]	2.741	0.7135
$R_\star$ [R$_\odot$]	2.0$\pm$0.2	1.17$\pm$0.17
$v \sin i$ [km.s^{-1}]	30.5$\pm$0.5	68.2$\pm$0.5
i [$^\circ$]	55$\pm$10	55$\pm$10
$P_{\rm orb}$ [d]	4.927$\pm$0.008	10.79$\pm$0.14
$M \sin i$ [M$_{\rm Jup}$]	0.57$\pm$0.10	1.66$\pm$0.31
a [au]	0.057$\pm$0.001	0.0968$\pm$0.0032
a [$R_\star$]	6.1$\pm$0.6	17.8$\pm$1.3

Table 1. Summary of the properties on both hot Jupiters found within the MaTYSSE programme. From top to bottom: age, stellar mass in terms of solar masses, stellar rotation period expressed, stellar radius in terms of solar radii, line-of-sight-projected equatorial rotation velocity, inclination of stellar rotation axis to the line of sight, orbital period, minimal mass in terms of jovian masses, semimajor axis and semimajor axis in terms of stellar radii.

that the planet did not dive into the star being explained by the presence of a magnetospheric gap at the center of the disc, caused by the magnetic field of the star (strong at a young age), and which stopped the migration from going further in.

It is not certain whether the position of the planets still mark the inner boundary of the discs at the time of dissipation, or if they have migrated due to tidal interactions in the meantime. If we assume them not to have migrated, the age of disc dissipation can be traced back by considering that the inner boundary was located at the corotation radius (due to magnetic coupling between the star and the disc), and thus finding the rotation rate of the star at the time of dissipation, leading to its age at that time by following evolutionary tracks.

If the planets have migrated however, it is important to study the star-planet system evolution by examining the interactions at play (magnetic, tidal), coupled with the temporal evolution of the stellar rotation rate, structure and magnetic field.

Finally, although the sample is still too small to be considered representative of actual statistics, finding 2 hJs in a sample of $\sim$30 stars bears the question of the frequency of hJs around young solar-like stars compared to that of hJs around mature ones (1%), and, rejoining the object of the previous paragraph, the dynamics that could lead to a potential decrease in hJ rate as star-planet systems evolve towards the main sequence.

Further observations will be conducted within both the MaTYSSE programme and the SPIRou (SpectroPolarimètre Infra-Rouge) Large Survey, enabling the community to ensure follow-up studies on the two detected hJs as well as refine our statistics on hJs around young solar-like stars. Our numerical methods are undergoing improvements in order to improve the modelling of the activity jitter, in particular by adding the intrinsic variability aspect into ZDI.

References

Donati, J.-F. & Brown, S. F. 1997, A&A, 326, 1135

Donati, J. F., Moutou, C., Malo, L., et al. 2016, Nature, 534, 662

Gregory, S. G., Donati, J.-F., Morin, J., et al. 2012, ApJ, 755, 97

Siess, L., Dufour, E., & Forestini, M. 2000, A&A, 358, 593

Yu, L., Donati, J.-F., Hébrard, E. M., et al. 2017, MNRAS, 467, 1342